Loss of DExD/H Box RNA Helicase LGP2 Manifests Disparate Antiviral Responses

Thiagarajan Venkataraman,[1]* Maikel Valdes,[1]* Rachel Elsby,* Shigeru Kakuta,† Gisela Caceres,* Shinobu Saijo,† Yoichiro Iwakura,† and Glen N. Barber[2]*

The DExD/H box RNA helicase retinoic acid-inducible gene I (RIG-I) and the melanoma differentiation-associated gene 5 (MDA5) are key intracellular receptors that recognize virus infection to produce type I IFN. A third helicase gene, *Lgp2*, is homologous to *Rig-I* and *Mda5* but lacks a caspase activation and recruitment domain. We generated *Lgp2*-deficient mice and report that the loss of this gene greatly sensitizes cells to cytosolic polyinosinic/polycytidylic acid-mediated induction of type I IFN. However, negative feedback inhibition of *IFN-β* transcription was found to be normal in the absence of LGP2, indicating that LGP2 is not the primary negative regulator of type I IFN production. Our data further indicate that $Lgp2^{-/-}$ mice exhibited resistance to lethal vesicular stomatitis virus infection, a virus whose replicative RNA intermediates are recognized specifically by RIG-I rather than by MDA5 to trigger the production of type I IFN. However, mice lacking LGP2 were observed to exhibit a defect in type I IFN production in response to infection by the encephalomyocarditis virus, the replication of which activates MDA5-dependent innate immune responses. Collectively, our data indicate a disparate regulatory role for LGP2 in the triggering of innate immune signaling pathways following RNA virus infection. *The Journal of Immunology,* **2007, 178: 6444–6455.**

Cellular detection of pathogenic microbes and activation of innate immune responses are now known to involve at least two main types of receptors. The first, referred to as the Toll-like receptors or TLRs have emerged as key surface molecules responsible for recognizing the conserved components of pathogenic microorganisms (referred to as pathogen-associated molecular patterns) (1, 2). The TLRs are evolutionarily conserved and play a key role in innate immune responses to Gram-positive bacteria in *Drosophila* (3, 4). At least 12 TLR members have now been identified in mammals (1). The TLRs are predominantly expressed on various immune cells in mammals such as macrophages and dendritic cells, and each TLR responds to a different pathogen-associated molecular pattern such as extracellular LPS (TLR 4), dsRNA (TLR 3), and single-stranded RNA (TLR 7/8) (1, 5). Following ligand binding, signaling pathways are initiated through an interaction with adaptor proteins harboring a Toll/IL-1R (TIR)[3] domain, which is also present in the cytosolic region of all TLRs (1, 5). TLRs such as TLR 2, 4, and 5 use a common adaptor protein referred to as MyD88, although alternate adaptor proteins referred to as TRIF/TICAM-1, TRAM, and TIRAP/Mal have also been now identified (1, 5–10). These adaptor proteins interact with members of the death domain-containing IL-1R-associated kinase (IRAK) family such as IRAK-1 and IRAK-4, which are serine-threonine kinases involved in the phosphorylation and activation of TNFR-associated kinase 6 (11–14). The stimulation of TLRs triggers common signaling pathways that culminate in the activation of the transcription factors NF-κB as well as the MAPKs ERK, p38, and JNK (1). In addition, the stimulation of TLR 3 or 4 can activate the transcription factor IFN-regulatory factor 3 (IRF-3) through TRIF-mediated activation of the noncanonical IκB kinase homologues IκB kinase-ε (IKKε) and TANK-binding kinase-1 (TBK1) (15, 16). Activation of the NF-κB-, ERK/JNK-, and IRF-3-responsive dsRNA signaling cascades culminates in the transcriptional stimulation of numerous genes such as the type I IFNs (15).

The TLR system, predominantly involving TLR 7 and 8, is essential for viral detection in plasmacytoid dendritic cells (17–19). However, alternate TLR-independent mechanisms of virus recognition and innate immune activation have recently been identified and reportedly involve a second type of intracellular receptor that belongs to the DExD/H box RNA helicase family. These helicases, referred to as the retinoic acid inducible gene I (RIG-I) and its homologue, melanoma differentiation-associated gene 5 (MDA5), contain a caspase activation and recruitment domain (CARD)/death-like domain (DLD) in their amino-terminal regions and have been reported as being able to trigger the production of type I IFN in response to virus infection (20, 21). For example, RIG-I has been shown to be essential for mediating the induction of type I IFN in response to negative-stranded viruses such as vesicular stomatitis virus (VSV), while MDA5 plays a more important role in the recognition of polyinosinic/polycytidylic acid (poly(I:C)) and

*Department of Microbiology and Immunology and Sylvester Comprehensive Cancer Center, University of Miami School of Medicine, Miami, FL 33136; and †Center for Experimental Medicine, Institute of Medical Science, University of Tokyo, Tokyo, Japan

Received for publication January 5, 2007. Accepted for publication February 28, 2007.

The costs of publication of this article were defrayed in part by the payment of page charges. This article must therefore be hereby marked *advertisement* in accordance with 18 U.S.C. Section 1734 solely to indicate this fact.

[1] T.V. and M.V. contributed equally to this work.

[2] Address correspondence and reprint requests to Dr. Glen N. Barber, University of Miami School of Medicine, 1550 Northwest 10th Avenue (M710), Papanicolaou Building, Room 511, Miami, FL 33136. E-mail address: gbarber@med.miami.edu

[3] Abbreviations used in this paper: TIR, Toll/IL-1R; IRAK, IL-1R-associated kinase; IRF, IFN-regulatory factor; DC, dendritic cell; BMDC, bone marrow-derived DC; CARD, caspase activation and recruitment domain; EMCV, encephalomyocarditis virus; FADD, Fas-associated death domain protein; IPS-1, IFN-β promoter stimulator 1; i.n., intranasal(ly); Luc, luciferase; MDA5, melanoma differentiation-associated gene 5; MEF, mouse embryonic fibroblast; MOI, multiplicity of infection; poly(I:C), polyinosinic/polycytidylic acid; qRT-PCR, quantitative RT-PCR; RIG-I, retinoic acid-inducible gene I; VSV, vesicular stomatitis virus; WT, wild type.

positive-stranded viruses such as the encephalomyocarditis virus (EMCV) (19, 22, 23). This may occur through the ability of RIG-I to specifically associate with viral single-stranded RNA, which contains 5′-phosphates such as those encoded by VSV (24, 25). In contrast, MDA5 appears to recognize longer dsRNA species such as those generated following EMCV infection. Reports indicate that RIG-I and MDA5 exert their activity through a recently identified CARD-containing molecule referred to as IFN-β promoter stimulator 1 (IPS-1). IPS-1 is also a potent inducer of type I IFN and a putative mitochondrial localized adaptor molecule required for MDA5 and RIG-I function (and also referred to as VISA, MAVS, and CARDIF) (26–29). In addition, the death domain-containing proteins FADD (Fas-associated death domain) and RIP1 play a role in regulating the induction of type I IFN and are required for efficient RIG-I, MDA5, and IPS-1 function (26, 30–32). A role for FADD and RIP1 in innate immune signaling pathways has similarly been demonstrated in *Drosophila* (3, 4). In this case, the *Drosophila* homologues of FADD and RIP1, referred to as dFADD and IMD, respectively, govern the activation of Relish (NF-κB) and the induction of antimicrobial genes in response to infection by Gram-negative bacteria (3, 4).

A third intracellular helicase, referred to as LGP2, exhibits extensive homology to MDA5 and RIG-I (41 and 31% respectively) but lacks amino-terminal CARD domains (32). Overexpression studies indicate that LGP2 does not appear to activate the production of type I IFN but rather may function as a negative feedback inhibitor of MDA5 and RIG-I, thus controlling dsRNA signaling events (32–34). It has been proposed that LGP2 may exert this activity through competitively sequestering dsRNA activators and/or by associating with components of the IFN-β signal transduction pathway (32, 34, 35). To further clarify the role of LGP2 in controlling intracellular dsRNA signaling pathways that govern the production of type I IFN, we have generated mice that lack a functional *Lgp2* gene. Our data indicate that *Lgp2*-lacking mice are viable, although they are significantly more sensitive to poly(I:C)-mediated production of type I IFN. Surprisingly, LGP2-deficient mice exhibited resistance to VSV infection but appeared sensitive to EMCV infection. This data may indicate disparate functions for LGP2 in the regulation of RIG-I and MDA5 activity and, accordingly, in the control of innate immune responses following infection with either negative- or positive-stranded viruses, respectively.

Materials and Methods

Construction of Lgp2 *knockout vector*

The genomic sequence of *Lgp2* was accessed through public domain databases (www.ensembl.org). Primers were designed to amplify 3-kb fragments upstream and downstream of exons 1–6 of the *D11LGP2*e gene. PCR was performed on 129Sv/J genomic DNA to amplify these two fragments using the following primers: upstream forward (5′-ATAAGAAATGC GGCCGCCTGAGCAGGTGTTGTACTAACTGAGCTCTACC-3′ and upstream reverse (5′-GACCAGGAGTCAGGAAATAGGCAGGCATTAAG-3′) and downstream forward (5′-CCATCGATCAGACACCCCAGAAG AGAGC-3′) and downstream reverse (5′-GACAGGGTCTCTCACTG AACC-3′).

The two fragments were cloned into plasmid vector pBL-Lx-Neo; the upstream fragment was cloned into *Not*I/*Sma*I sites and downstream fragment into *Cla*I/*Hin*cII sites flanking either side of the pGK-Neo cassette. *Not*I and *Cla*I sites were added to the primers. *Sma*I cloning was accomplished by ligation with the blunt 3′ end of the PCR fragment. The 3′ *Hin*cII of the downstream fragment was an internal site 31 bases upstream of the downstream reverse primer.

Generation of the Lgp2 *knockout mice*

The linearized targeting vector was electroporated into E14.1 embryonic stem cells originated from 129SvEv strain, followed by the selection in G418. Targeted clones were screened by PCR and Southern blot hybridization as described below. From 50 clones, one positive clone was identified. This embryonic stem cell clone was subjected to the generation of chimera mice by injection using C57BL/6J blastocysts as the hosts. The resulting male chimeras were further mated with C57BL/6J female mice for germline transmission. The heterozygous mice (F1 mice) were interbred to obtain wild-type (WT), heterozygous, and homozygous littermates (F2); the following generations (F3 and F4) were in a mixed 129SvEv/C57BL6J (50%/50%) genetic background. The genotypes of the mice were determined by PCR and Southern blot analysis of genomic DNA obtained from the tails as described below. Animals were generated at the University of Miami School of Medicine Transgenic Core Facility (Miami, FL). Mice were allowed to freely access food and water and were housed at an ambient temperature of 23°C and at a 12-h light/dark cycle. Animal care and handling was performed as per Institutional Animal Care and Use Committee guidelines.

Isolation and primary culture of mouse embryonic fibroblasts (MEFs)

Primary MEF cultures were established from embryos produced by intercrossing heterozygous mutant mice. Mice from the F2 generation were paired up for mating and the formation of the vaginal plug was monitored and designated as day 0. After 13.5 days post coitum, pregnant female mice were sacrificed and embryos dissected. Embryos were cut, excluding the brain and the liver; the rest of the fetus was minced with a sterile razor blade into small pieces, incubated in 0.05% trypsin and 0.02% EDTA at 37°C for 30 min with periodic agitation, dispersed by pipetting, and passed through a 40-μm cell strainer. Cells were grown in high glucose DMEM (Invitrogen Life Technologies) containing 10% FBS (Invitrogen Life Technologies) and 0.1 mg/ml Primocin (Amaxa Biosystems) until confluent. The excised brain and liver tissues were frozen at −80°C for genotype confirmation by PCR.

Cells, viruses, and reagents

MEFs were obtained from the following sources: *STAT1*$^{+/+}$ and *STAT1*$^{-/-}$ MEFs (J. Durbin, Children's Hospital, Columbus, OH). VSV-WT (Indiana strain) and EMCV were purchased from American Type Culture Collection. Poly(I:C) (Amersham Biosciences) was reconstituted in PBS at 2 mg/ml, denatured at 55°C for 30 min, and allowed to anneal at room temperature before use. Unless indicated otherwise, MEFs were transfected with 6 μg of poly(I:C) in 8 μl of Lipofectamine 2000 (Invitrogen Life Technologies) to stimulate promoter activation and IFN production. Murine IFN-α and -β ELISA kits and anti-IFN-α and -β Abs were acquired from PBL Biomedical Laboratories. All other reagents were from Sigma-Aldrich unless noted otherwise.

Plasmids

Expression vectors (pcDNA3-Neo; Invitrogen Life Technologies) encoding FLAG-tagged versions of human RIG-I and MDA-5 were generated by PCR. Plasmid pBL-Lx-Neo-DT, based on a pBluescript SK$^-$ backbone (Stratagene), has been previously described (36). A downstream diphtheria toxin expression module facilitated a high percentage of homologous recombination events.

Antibodies

Abs were obtained from the following sources: Abs to LGP2 and RIG-I were a gift of T. Fujita (Kyoto University, Kyoto, Japan; Ref. 20). Ab to MDA5 was a gift from P.B. Fisher (Columbia University College of Physicians and Surgeons, New York, NY; Ref. 21). CD11c-FITC, CD86-PE, and CD83-PE were purchased from BD Biosciences.

Preparation of dendritic cells (DCs) and macrophages

Bone marrow-derived DCs (BMDCs) were prepared from femurs and tibia isolated from WT and knockout mice. A single cell suspension (per mouse) was prepared and RBCs were lysed. Cells were cultured in DMEM supplemented with 10% FCS, 50 μM 2-MR, 100 U/ml penicillin, 100 μg/ml streptomycin, and 20 ng/ml GM-CSF. Medium was replaced every 2 days. On day 6, cells were purified using MACS separator CD11c (N418) microbeads (Miltenyi Biotec) following the manufacturer's instructions. After maturation, DCs were stimulated with either mock, VSV or EMCV treatment. After 24 h of treatment, cells were analyzed for surface marker expression by FACS. DCs (10^5) were stained with 1 μg of CD11c-FITC, CD86-PE, or CD83-PE for analysis.

Macrophages from WT and LGP2e$^{-/-}$ mice were collected 4 days after intraperitoneal thioglycollate injection (2 ml of 3% thioglycollate) by

washing the peritoneal cavity with HBSS and collecting the peritoneal exudate cells. The collected cells were cultured in DMEM with 10% FBS and penicillin/streptomycin and allowed to adhere in flat-bottom 48 well plates. Cells were infected with VSV at a multiplicity of infection (MOI) of 10. After 24 h, cell culture supernatants were collected and viral titers were determined by a standard plaque assay in baby hamster kidney cells.

DNA microarray analysis

Total RNA was extracted from MEFs stimulated in a 10-cm dish with or without poly(I:C) (6 μg/ml in Lipofectamine 2000) or VSV-GFP (MOI of 5.0). The preparation of mRNA and microarray analysis was performed at the W.M. Keck Foundation Biotechnology Research Laboratory DNA microarray facility at Yale University (New Haven, CT). The mouse genome 430-2.0 array (Affymetrix) was used. Data analysis was performed with GeneSpring software (Silicon Genetics).

Real-time PCR

Total RNA was isolated from samples using the RNeasy RNA extraction kit (Qiagen) and cDNA synthesis was performed using 1 μg of total RNA (Roche). Fluorescence real-time PCR analysis was performed using a LightCycler 2.0 instrument (Roche) and TaqMan gene expression assays (Applied Biosystems). Relative amounts of mRNA were normalized to the 18S ribosomal RNA levels in each sample.

Virus infections

MEF cells were plated in 12-well plates at 100,000 cells/well and allowed to adhere overnight. They were infected with recombinant VSV expressing GFP, VSV-WT, or EMCV. Supernatants were collected at different time points and the viral progeny yield was measured by standard plaque assay on baby hamster kidney cells.

NF-κB ELISA

To detect active p65 containing NF-κB complexes, the EZ-Detect NFκB p65 transcription factor kit (Pierce) was used. The manufacturer's recommended protocol was used to assay for activation of NF-κB. Samples were collected and lysed in radioimmune precipitation assay buffer containing protease inhibitors and an assay was conducted according to assay protocol. Values are graphed as a fold relative to the mock or h 0 time point samples.

Cytokine profiling

IFN-α and IFN-β were detected in cell-free supernatant and mice sera by ELISA (PBL Biomedical Laboratories). IFN-γ and IL-12 were measured using the BD cytometric bead array (BD Biosciences). Other cytokines were measured by the TranSignal mouse cytokine Ab array (Panomics). All protocols were performed as per the manufacturer's recommendations.

In vivo imaging of mice

Mice were infected intranasally (i.n.) with VSV expressing luciferase (Luc) at 10^7 PFU/mouse in a 10-μl volume (5 μl per nostril). On different days after the initial infection the progression of infection was monitored. Animals were anesthetized and injected with luciferin (150 mg/kg) 5 min before bioluminescence imaging. Animals were placed on a warmed stage (37°C) and imaged using an IVIS 200 system (Xenogen). Bioluminescence was monitored by detecting photon emission using a charge-coupled device camera. Images of infected mice were displayed as a pseudo-color image representing light intensities superimposed over the white light image of the body surface.

Statistical analysis

Statistical significance of differences in cytokine levels, viral titers, and luciferase intensity in VSV-Luc-infected mice was determined using Student's *t* test. Survival curves were analyzed using the logrank test.

Results

Generation of Lgp2$^{-/-}$ mice

To elucidate the function of the DExD/H box helicase LGP2, in vivo, we developed *Lgp2*-deficient (*Lgp2*$^{-/-}$) mice by targeted homologous recombination in embryonic stem cells (Fig. 1*A*). The deletion of *Lgp2* was confirmed by Southern and Northern analyses as well as by RT-PCR analysis (Fig. 1, *B* and *C*, and data not shown). *Lgp2*$^{-/-}$ animals were born at the Mendelian ratio and developed and bred normally (Fig. 1*D*). MEFs derived from *Lgp2*$^{-/-}$ fetuses were treated with type I IFN and immunoblot analysis was conducted using an anti-LGP2 antiserum, the results of which verified that the LGP2 protein is indeed lacking in these cells (Fig. 1*E*). This study further confirmed that LGP2 is not abundantly expressed in MEFs in the absence of type I IFN. Microarray and immunoblot analysis of normal MEFs confirmed that LGP2 as well as RIG-I and MDA5 are efficiently up-regulated following exposure to both type I and II IFN (Fig. 1, *E* and *F*). However, *Mda5* and to a lesser extent *Rig-I* were also found to be transcriptionally activated in a STAT1-independent manner, indicating that they additionally lie in the primary innate immune response pathway (Fig. 1, *G* and *H*). *Lgp2*, in contrast, appears to be predominantly synthesized in a STAT1-dependent manner. Thus, following exposure to intracellular poly(I:C), *Lgp2* would presumably be synthesized in an autologous manner after the production of MDA5 and RIG-I and the induction of *IFN-β*.

Enhanced poly(I:C)-mediated induction of type I IFN in LGP2$^{-/-}$ cells

It has been reported that LGP2 is a potential dominant negative regulator of RIG-I and MDA5 activity and can function to inhibit poly(I:C)-mediated, TLR-independent synthesis of type I IFN (20). To therefore investigate the role of LGP2 in poly(I:C) signaling events, we transfected *Lgp2*$^{-/-}$ MEFs with poly(I:C) and examined the production of *IFN-β* mRNA and protein by RT-PCR, microarray analysis, and ELISA. These studies indicated that endogenous *IFN-β* mRNA was up-regulated several hundred-fold in the absence of LGP2, compared with controls, at 3 and 6 h posttreatment (Fig. 2*A*). Similarly, the induction of *IFN-α2* mRNA, which is largely dependent on IFN-β-mediated STAT1-regulation, was found to be elevated in *Lgp2*$^{-/-}$ MEFs compared with WT cells (Fig. 2*B*). These findings were corroborated by ELISA studies confirming that the IFN-β and -α protein levels were increased several-fold in *Lgp2*$^{-/-}$ cells compared with controls by 6–12 h posttreatment (Fig. 2, *C* and *D*). Microarray mRNA expression profiles of poly(I:C)-treated *Lgp2*$^{-/-}$ or *Lgp2*$^{+/+}$ MEFs demonstrated that the mRNA levels of a number of dsRNA-inducible genes such as *IL-6* and *IFN-α4* are also enhanced by poly(I:C) early after treatment in the absence of LGP2 (Fig. 2*E*). Additional examination verified that NF-κB activity was augmented in *Lgp2*$^{-/-}$ cells compared with control cells following exposure to intracellular poly(I:C) (Fig. 2*F*). Thus, the loss of LGP2 results in the enhanced synthesis of genes regulated by transfected poly(I:C).

To start to evaluate the in vivo role of LGP2 in mediating dsRNA signaling events, we inoculated animals deficient in LGP2 or controls with poly(I:C) and monitored type I IFN production at 6 and 12 h posttreatment. These data indicated that the levels of dsRNA-mediated IFN-β and -α production did not significantly vary in the presence or absence of LGP2 (Fig. 2*G*). A further evaluation of cytokine production in response to poly(I:C) was conducted using murine cytokine Ab array analysis. Although RANTES was found to be moderately enhanced in the control cells, this study similarly indicated no significant differences in general cytokine levels in *Lgp2*$^{-/-}$ mice compared with controls following i.v. inoculation with poly(I:C) (Fig. 2*H*). Thus, the loss of LGP2 does not seem to significantly affect the in vivo production of type I IFN following exposure to exogenous poly(I:C), presumably because these events are largely modulated by the TLR pathway, which is independent

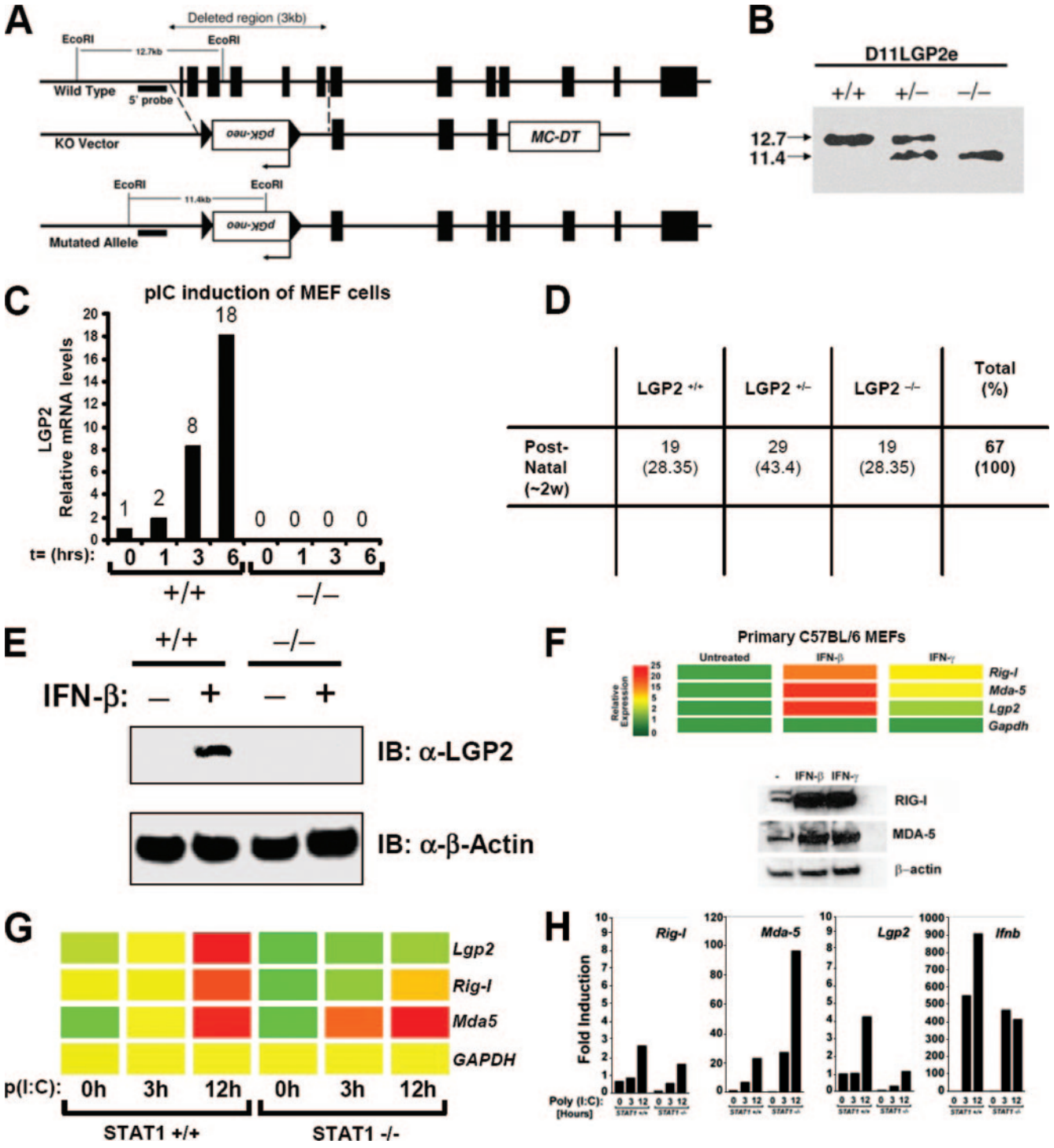

FIGURE 1. Generation of *Lgp2*$^{-/-}$ mice. *A*, Structure of the murine *Lgp2* gene, targeting vector, and the predicted disrupted gene. Filled in boxes denote exons. Six exons were deleted, including the ATG start codon. MC-DT denotes diphtheria toxin selection cassette *B*, Southern blot analysis of *Eco*R1-digested DNA from murine tails using the 5′-probe as shown in *A*. A 12.7-kb band for *Lgp2*$^{+/+}$ and 11.4-kb band for *Lgp2*$^{-/-}$ offspring are expected. *C*, RT-PCR analysis of *Lgp2* mRNA in type I IFN-treated MEFs from WT or *Lgp2* knockout embryos. *D*, Genotype analysis of intercrossed neonatal *Lgp2*$^{+/-}$ offspring. *E*, Immunoblot analysis of protein extracts from MEFs treated with or without type I IFN using an Ab to LGP2 or actin. *F*, Microarray and immunoblot (IB) expression analysis of RIG-I and MDA5 in IFN-treated MEFs. *G*, The induction of *Rig-I*, *Mda5*, and *Lgp2* in poly(I:C)-transfected *STAT1*-deficient cells. *H*, Confirmation of *G* by qRT-PCR.

of RIG-I/MDA5 and LGP2 function (15). These data also indicate that the inhibition of IFN-β production in response to exogenous dsRNA species is not dependent on LGP2 (Fig. 2*G*).

To extend these studies, we next examined whether RIG-I or MDA5 directly exerted any enhanced ability to stimulate the production of type I IFN in the absence of LGP2. Following the transfection of heterologous MDA5 or RIG-I into control or *Lgp2*$^{-/-}$ MEFs, we found that endogenous *IFN-*β production was stimulated >200-fold in the absence of LGP2, further suggesting that this latter helicase may indeed exhibit a negative regulatory role on early transfected dsRNA-mediated type I IFN production (Fig. 3*A*). Similar effects were seen to occur with STAT1-dependent

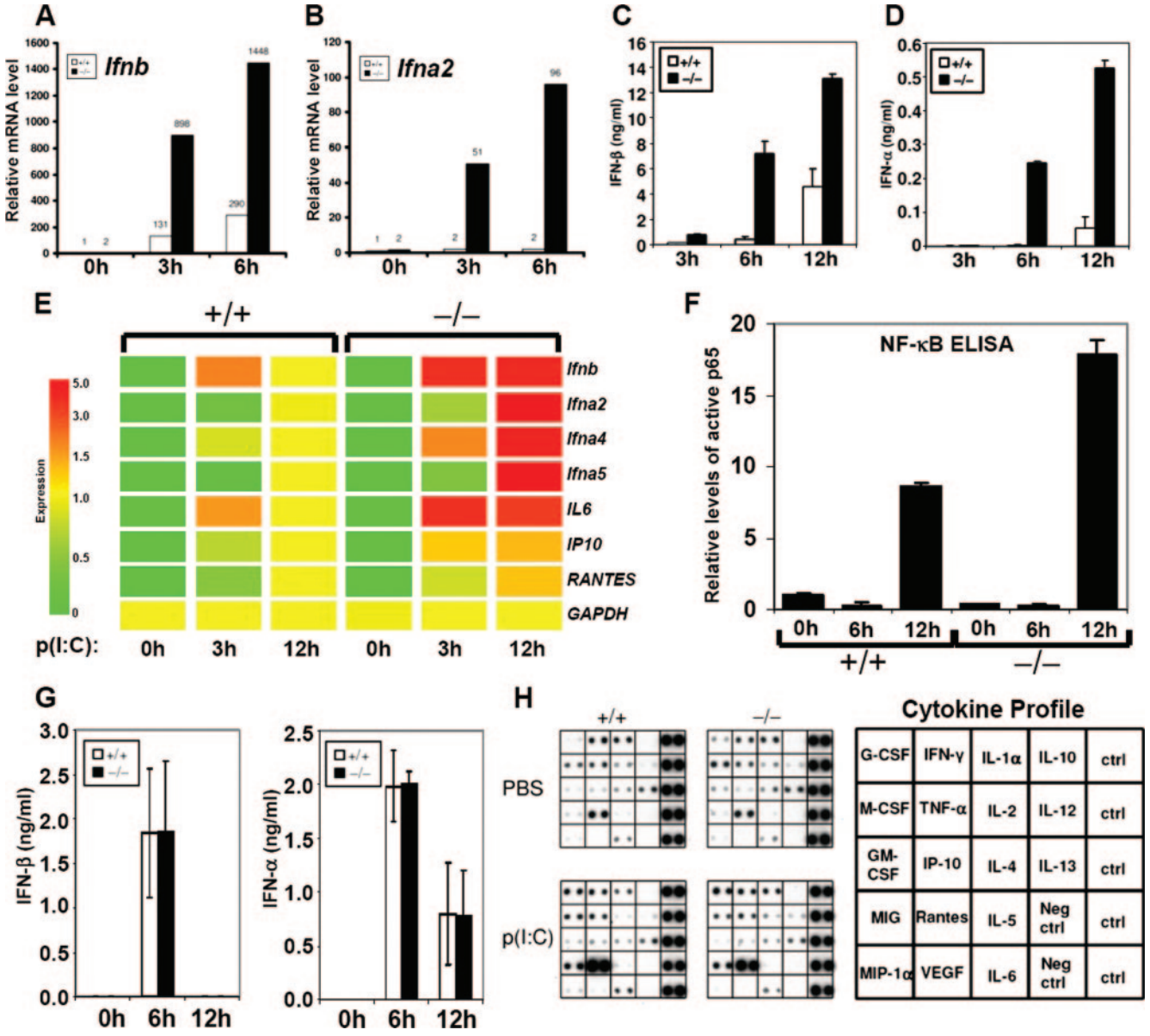

FIGURE 2. The regulation of poly(I:C) signaling in the absence of LGP2. *A*, Analysis of *IFN-β* (*Ifnb*) mRNA induction by qRT-PCR in control or $Lgp2^{-/-}$ cells transfected with poly(I:C) (6 μg/ml in Lipofectamine 2000) for the indicated time points. The mRNA levels are expressed as a fold relative to the $Lgp^{+/+}$ sample at the h 0 time point. *B*, Analysis of *IFN-α2 (Ifna2)* mRNA induction by qRT-PCR in control or $Lgp2^{-/-}$ cells transfected with poly(I:C) for indicated time points. *C*, Analysis of IFN-β protein production by ELISA from medium harvested from control or $Lgp2^{-/-}$ cells transfected with poly(I:C) at the indicated time points. *D*, Analysis of IFN-α protein production by ELISA from medium harvested from control or $Lgp2^{-/-}$ cells transfected with poly(I:C) at the indicated time points. *E*, Microarray analysis of *Rig-I*, *Mda5*, or *Lgp2* mRNA expression in poly(I:C)-transfected (6 μg/ml complexed in Lipofectamine 2000) WT MEFs at the indicated time points. Samples were normalized to *GAPDH* expression levels and to the expression levels in $Lgp2^{+/+}$ cells at 12 h. *F*, Increased NF-κB signaling in $Lgp2^{-/-}$ cells transfected with poly(I:C) as described above. Equal amounts of protein extract (10 μg) were examined by ELISA to measure active p65. Fold activity is depicted relative to h 0 in $Lgp2^{+/+}$ cells. *G*, Type I IFN production in $Lgp2^{-/-}$ mice injected i.v. with noncomplexed poly(I:C). Following inoculation of mice ($n = 4$) with 200 μg poly(I:C), serum was collected and IFN-β and -α levels were measured by ELISA. *H*, Cytokine profiles of mice inoculated with 200 μg poly(I:C), as in *G*. Analysis was done in duplicate per group and the results of one typical experiment (6 h posttreatment) are shown.

IFN-α2 mRNA, presumably due to the abundance of IFN-β being prevalent (Fig. 3*B*). Finally, the type I IFN inducer IPS-1 also appeared unaffected in LGP2-lacking cells (Fig. 3*C*).

To complement this study, we pretreated cells with type I IFN. This was done because our analyses had indicated that, in the absence of type I IFN, the expression levels of LGP2 are low. Following exposure to type I IFN, however, endogenous levels of LGP2 would increase (Fig. 1*D*). To thus examine whether the increased presence of endogenous LGP2 exerted an influence on the production of IFN-β in response to intracellular dsRNA, we measured the induction of *IFN-β* mRNA in $Lgp2^{-/-}$ or control cells pretreated with type I IFN. Fig. 4*A* indicates that the production of *IFN-β* mRNA was significantly enhanced in $Lgp2^{-/-}$ cells compared with controls in either IFN-treated and untreated MEFs following exposure to intracellular poly(I:C). However, the induction of type I IFN by intracellular dsRNA species characteristically declined between 6 and 12 h poststimulation in both the $Lgp2^{+/+}$ and $Lgp2^{-/-}$ MEFs (19). This effect also occurred in the type I IFN-treated cells. These data

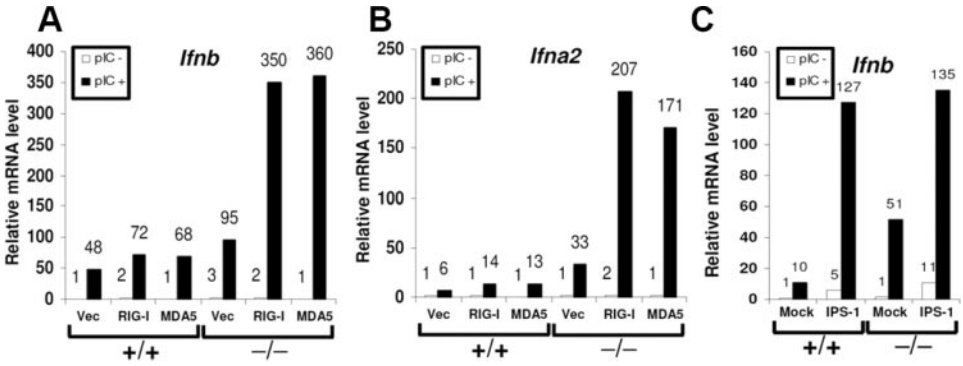

FIGURE 3. Analysis of *Rig-I*, Mda5, and *IPS-1* expression in the absence of LGP2. *A*, Analysis of *Rig-I* and *Mda5* function in *Lgp2*$^{-/-}$ MEFs. *Lgp2*$^{-/-}$ cells or controls were transfected with heterologous *Rig-I* or *Mda5* for 30 h before treatment (3 h) with (pIC +) or without (pIC −) poly(I:C) (6 μg/ml in Lipofectamine 2000). *IFN-β* (*Ifnb*) mRNA levels were determined using qRT-PCR and are depicted as a fold increase relative to the vector (Vec)-treated *Lgp*$^{+/+}$ sample without poly(I:C). *B*, Analysis of *IFN-α2* (*Ifna2*) mRNA production from the experiment in A. *C*, Analysis of *IPS-1* function in *Lgp2*$^{-/-}$ MEFs. *Lgp2*$^{-/-}$ cells or controls were transfected with heterologous *IPS-1* for 30 h before treatment (3 h) with or without poly(I:C) (6 μg/ml in Lipofectamine 2000). *IFN-β* (*Ifnb*) mRNA levels were determined using qRT-PCR and are depicted as a fold increase relative to mock treated *Lgp2*$^{+/+}$ sample, without poly(I:C).

would suggest that LGP2 does not exert significant influence as a negative feedback inhibitor on MDA5 or RIG-I activity, because LGP2 is obviously absent in the *Lgp2*$^{-/-}$ MEFs and yet the decline of *IFN-β* mRNA in response to poly(I:C) typically diminishes. Fig. 4, *B* and *C* (*lower panels*) ensured that IFN-β induction of IFN-stimulated response element (ISRE)-stimulated genes occurs in *Lgp2*$^{-/-}$ cells and that the IRF-7 and RIG-I proteins were prevalent at 3–12 h posttransfection and thus not a cause for a reduction in *IFN-β* transcription. Thus, although the loss of LGP2 facilitates RIG-I/MDA5 activity mediated by poly(I:C) early after transfection, the mechanism for negative feedback inhibition of type I IFN is likely LGP2 independent.

Antiviral responses in LGP2 lacking MEFs

To determine whether the loss of LGP2 affected antiviral innate immune signaling responses, we infected the control or *Lgp2*$^{-/-}$ MEFs with VSV, a single, negative-stranded RNA virus and member of the *Rhabdoviridae* family, and monitored the production of type I IFN. RIG-I, rather than MDA5, has been reported as being essential for the production of type I IFN in response to VSV infection (19). Our data indicated that the stimulation of *IFN-β* mRNA by VSV was significantly less compared with the stimulation by transfected poly(I:C), presumably because VSV is able to conceal its RNA from interacting with dsRNA stress sensors such as RIG-I (19). Further, an encoded VSV M protein would prevent the export of *IFN-β* mRNA required for positive feedback enhancement of additional RIG-I and MDA5 as well as IRF-7, which bolsters IFN-β production (37). However, slightly elevated production of IFN-β and IFN-α2 mRNA was again observed in *Lgp2*$^{-/-}$ cells compared with controls as initially determined by quantitative RT-PCR (qRT-PCR) analysis following infection with VSV (Fig. 5, *A* and *B*). The effect was confirmed following microarray analysis of VSV-infected *Lgp2*$^{-/-}$ or control MEFs (Fig. 5*C*). Although the induction of type I IFN is low, these data are consistent to those obtained using transfected poly(I:C) and would

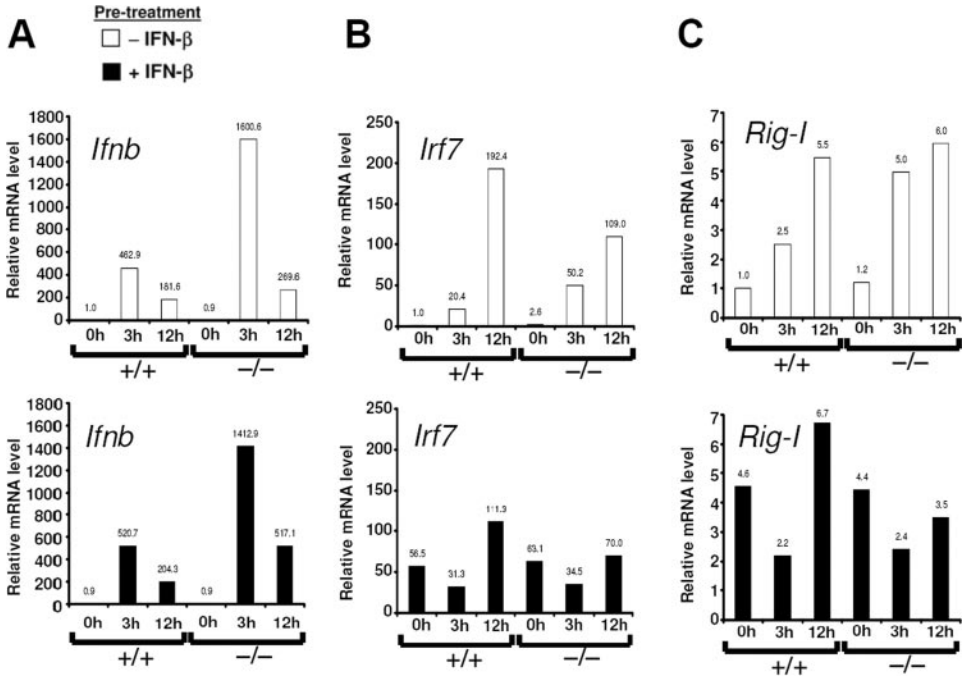

FIGURE 4. The effect of IFN-β pretreatment on poly(I:C) signaling in *Lgp2*$^{-/-}$ MEFs. *A*, *Lgp2*$^{-/-}$ or controls were pretreated with (filled histogram) or without (unfilled histogram) 20 U/ml murine IFN-β for 16 h. Cells were then transfected with poly(I:C) for the indicated times and mRNA for *IFN-β* measured by qRT-PCR. mRNA levels are expressed as the fold induction relative to the untreated *Lgp2*$^{+/+}$ sample at h 0. *B*, *Irf7* mRNA measurements from experiment in *A*. *C*, *Rig-I* mRNA measurements.

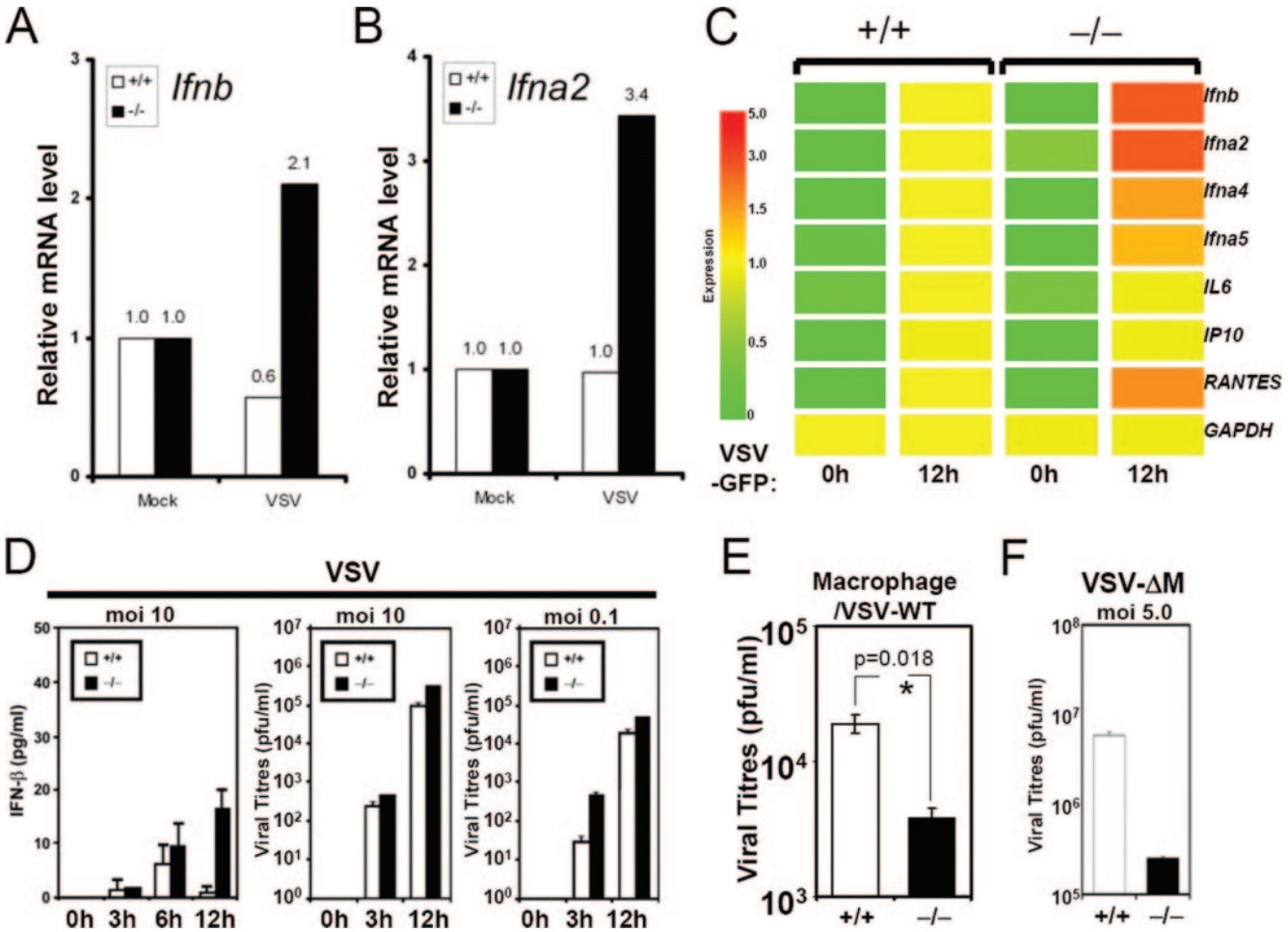

FIGURE 5. The regulation of type I IFN induction by VSV. *A*, Analysis of the induction of *IFN-β* mRNA by qRT-PCR in control or $Lgp2^{-/-}$ cells infected with VSV (Indiana Strain; MOI of 0.1) 12 h postinfection. The mRNA levels are expressed as fold induction relative to the $Lgp^{+/+}$ sample mock treated. *B*, Analysis of IFN-stimulated response element-inducible *IFN-α2* mRNA from as described in *A*. *C*, Microarray mRNA analysis of innate immune response genes in $Lgp2^{-/-}$ or control MEFs infected with VSV (MOI of 5 for the times indicated). Samples were normalized to GAPDH expression levels and to the expression levels in $Lgp2^{+/+}$ cells at 12 h. *D*, Analysis of IFN-β protein by ELISA from the medium of control or $Lgp2^{-/-}$ cells infected with VSV (Indiana Strain; MOI of 10) for the indicated time points. Viral titers from the same supernatant (MOI of 10) and from cells infected at MOI of 0.1 were measure by plaque assay. *E*, Thioglycollate-induced peritoneal macrophages were isolated, cultured, and infected with VSV (MOI of 10) for 24 h. Supernatants were collected and viral titers were measured by plaque assay. Statistical significance was measured by Student's *t* test. *F*, $Lgp2^{-/-}$ or control MEFs were infected with VSV M 52–54 at MOI of 5. Supernatant was collected after 24 h and viral titers were measured by a standard plaque assay.

again suggest that LGP2 exerts an inhibitory effect on at least RIG-I signaling, which is essential for the recognition of VSV-related RNA. ELISA analysis of IFN-β protein production indicated that the levels of these cytokines were slightly elevated in LGP2-lacking MEFs following VSV infection (Fig. 5*D*). Presumably the low levels of IFN production reflect the ability of these viruses to inhibit the production of cellular protein after infection by various mechanisms (37). To complement this study, we examined viral replication in MEFs lacking or containing LGP2 and found that there were approximately equivalent levels of VSV produced at MOI values of 10 and 0.1 (Figs. 5*D*). Plausibly, the small amount of IFN made in vitro in MEFs, even in the absence of LGP2, in response to infection is insufficient to dramatically affect viral titers. To extend this study, we examined the replication of VSV in macrophages and found that a loss of LGP2 leads to slightly decreased viral replication (Fig. 5*E*). To complement this approach, a VSV mutant virus was generated that encoded a defective M protein (VSV-M 52–54) (37). This virus is unable to inhibit IFN-β mRNA export and, thus, type I IFN transcription and translation are increased through autologous feedback mechanisms. In this situation, VSV-M 52–54 replicated to significantly lower titers in MEFs lacking LGP2 (Fig. 5*F*). Thus, whereas the loss of LGP2 seems to augment the production of type I IFN mRNA in response to virus infection, the effects observed are not as dramatic as those obtained using transfected poly(I:C), in part due to the probable viral evasion of host defense. However, cells lacking LGP2 appear to exhibit slight resistance to VSV infection in vitro.

Mice lacking LGP2 are more resistant to VSV infection

To investigate the role of LGP2 in antiviral responses in vivo, we inoculated control or $Lgp2^{-/-}$ mice with 1×10^5 or 1×10^7 VSV (Indiana strain) i.n. and monitored survival. As shown in Fig. 6*A*, all but one WT animal succumbed to virus infection by 9 days postinoculation at 10^7 pfu, and 40% of the animals died at 10^5 pfu. However, mice lacking LGP2 exhibited resistance to VSV infection and only two animals succumbed by day 7 following i.n. exposure at 10^7 PFU. None of the $Lgp2^{-/-}$ animals died following exposure to 10^5 PFU. No further animals from either group died after the indicated time points. In a separate

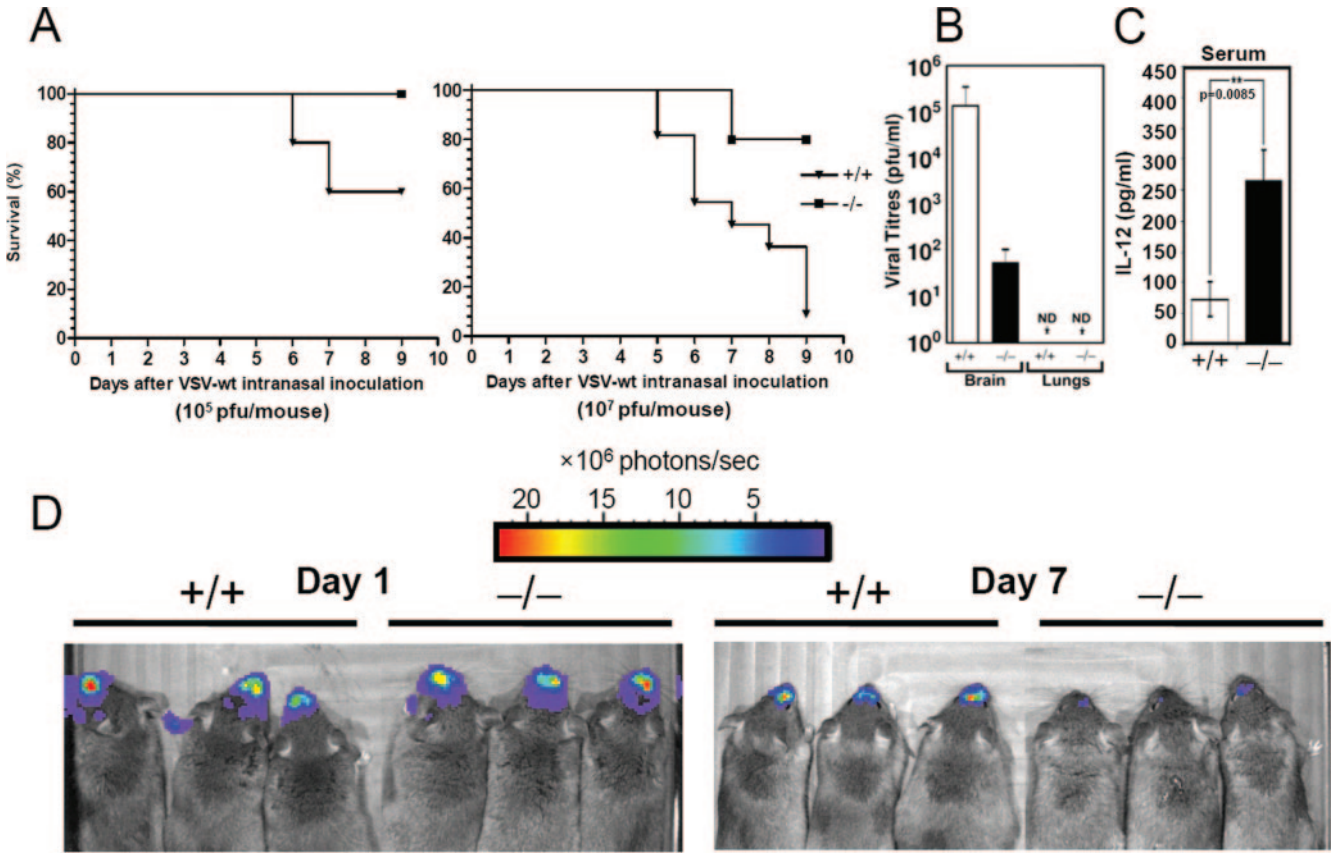

FIGURE 6. Infection of *Lgp2*$^{-/-}$ mice with VSV. *A*, Survival of *Lgp2*$^{-/-}$ or control mice ($n = 10$, 5 wk old) infected i.n. with VSV (10^5 and 10^7 Indiana strain). *B*, *Lgp2*$^{-/-}$ or control mice were infected with 10^7 pfu of VSV i.n. Mice ($n = 5$) and sacrificed after day 7 and viral titers measured in the brains and lungs. *C*, Control or *Lgp2*$^{-/-}$ mice ($n = 3$) were infected with VSV as described above and after 5 days the serum was collected and IL-12 levels were measured by bead array. The probability of error was measured by Student's *t* test. *D*, Control or *Lgp2*$^{-/-}$ mice ($n = 3$) were infected intranasally with VSV-Luc. After the indicated time in days the mice were anesthetized and injected i.p. with a luciferin substrate and Luc activity was detected using the IVIS imaging system (Xenogen). A pseudocolor image of areas showing luciferase expression is superimposed over a white light image of the body surface to indicate the areas where VSV-Luc is present.

experiment, control or *Lgp2*$^{-/-}$ animals were infected with 10^7 PFU of VSV i.n. and sacrificed on day 6. Brain and lung tissue was retrieved and examined for viral titers. This analysis indicated significantly higher levels of VSV in the brains of control but not *Lgp2*$^{-/-}$ mice (Fig. 6*B*). No virus was detected in the lungs of either animal. An analysis of serum taken from animals at day 5 indicated high levels of IL-12 production in *Lgp2*$^{-/-}$ mice compared with controls, indicative of enhanced adaptive immune responses at this time period (Fig. 6*C*). To complement this study, we infected (i.n. at 10^7 PFU) mice lacking LGP2 or control animals with an attenuated recombinant VSV-Luc. In vivo luminescence analyses at day 1 postinfection revealed the replication of VSV-Luc in the nasal region of both control and *Lgp2*$^{-/-}$ mice (Fig. 6*D*). However, at day 7 significantly less luciferase was evident in mice lacking LGP2 compared with controls, indicating more robust clearance of the virus in accordance with data shown in Fig. 6*A* ($p = 0.0076$ by unpaired *t* test).

Plausibly, resistance to VSV may involve an enhanced ability to trigger the production of type I IFN in the absence of LGP2, which may exert an antiviral effect. To explore this possibility, we inoculated control or *Lgp2*$^{-/-}$ mice i.n, with VSV (1×10^5) and examined the animals for type I IFN production 5 days postinfection. Analysis of type I or II IFN levels in the serum of animals at this time point did not reveal any detectable quantities of these cytokines in the control or *Lgp2*$^{-/-}$ mice, plausibly because the infection had largely been contained in the olfactory region by this time point (data not shown). However, as mentioned, significant quantities of IL-12, which has been proposed to facilitate recovery from viral encephalitis, were observed by day 5 in mice lacking LGP2 (day 5, 10^5 VSV; Fig. 6*C*) (38). Serum taken from animals infected i.n. (day 7, 10^7 VSV-WT) were next examined for selected cytokine expression by immunoblotting revealing that VSV-infected WT mice exhibited slightly higher levels of G-CSF, M-CSF, and TNF-α, indicative of inflammatory reaction in the presence of virus infection (Fig. 7*C*). This was more evident when analyzing homogenized brain extracts of infected animals. In this case, significant amounts of both IFN-β and -α were observed by ELISA in WT animals but not *Lgp2*$^{-/-}$ mice because viral replication was occurring predominantly only in the brains of control animals at this time point (Figs. 6*B* and 7, *A* and *B*). Cytokine profile analysis also indicated the presence of high levels of proinflammatory proteins such as the IP-10 (IFN-γ-inducible protein, 10 kDa) in control animals compared with *Lgp2*$^{-/-}$ mice. Collectively, these data would indicate that LGP2$^{-/-}$ animals clear virus infection more evidently than WT animals and avoid the inflammation typical of encephalitis mediated by virus infection.

To complement this study, we inoculated *Lgp2*$^{-/-}$ or control mice i.v. with VSV (1×10^7) and measured cytokine responses earlier, at 6 and 24 h postinfection. These data revealed slightly

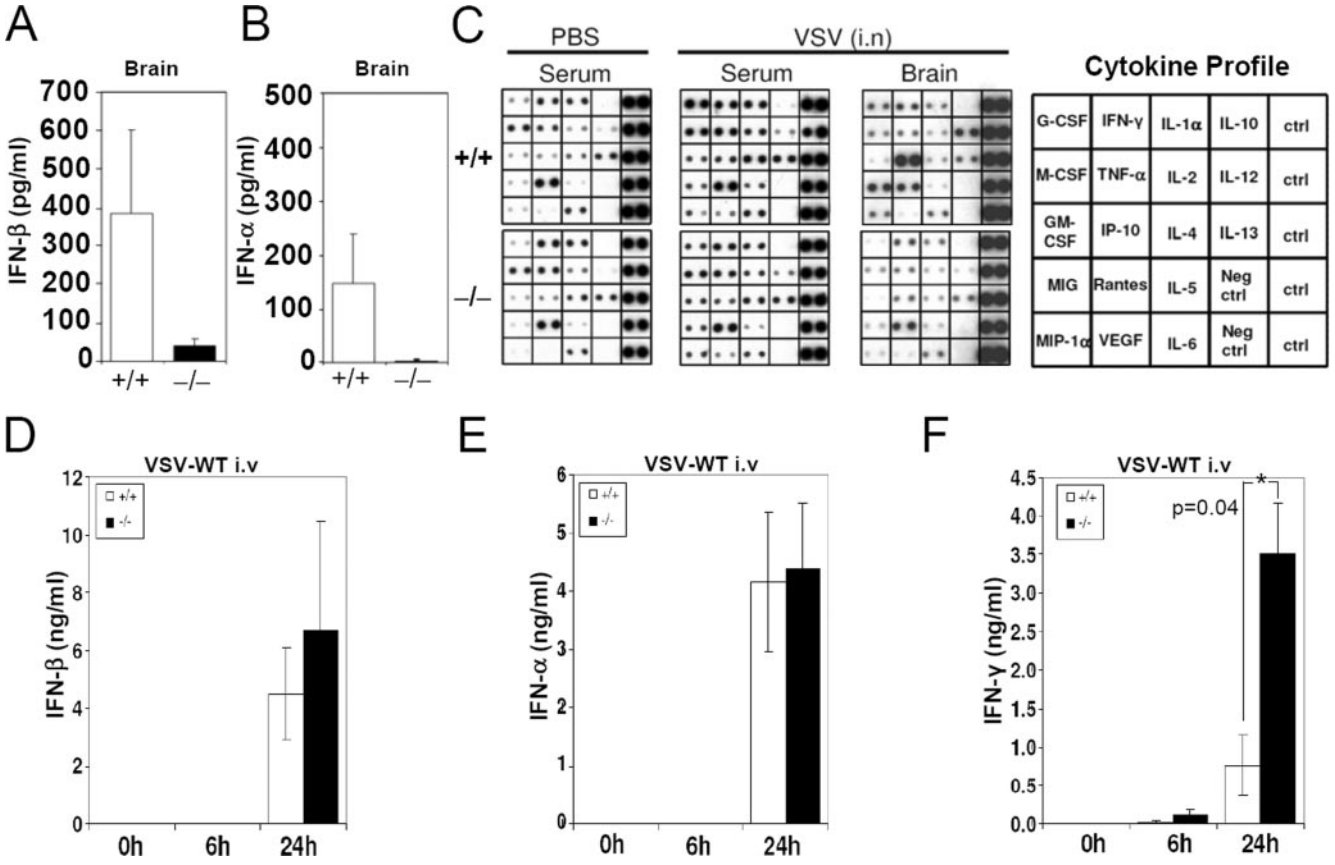

FIGURE 7. Cytokine profile of $Lgp^{-/-}$ mice infected with VSV. *A*, Control or $Lgp2^{-/-}$ mice were infected intranasally with VSV (10^7 PFU/mouse, $n = 5$) and sacrificed after day 7. IFN-β levels were measured in brain lysates by ELISA. *B*, IFN-α levels were measured by ELISA in the same samples as in *A*. *C*, Cytokine profiles of mice infected with 10^7 pfu of VSV i.n. Mice were sacrificed at day 7 and serum and brain lysates were collected for analysis. Analysis was done in duplicate per group and the results of one typical experiment are shown. *D*, Control or $Lgp2^{-/-}$ mice ($n = 3$) were inoculated i.v. with VSV (10^7, Indiana strain) and IFN-β levels were measured by ELISA from serum taken at the indicated time points. *E*, As in *C* above, except that IFN-α was measured. *F*, As in *C* above except that IFN-γ was measured using cytometric bead array.

more IFN-β induction in $Lgp2^{-/-}$ animals compared with controls at 24 h postinoculation, although IFN-α levels remained similar (Fig. 7, *D* and *E*). More significantly, IFN-γ levels were considerably higher in mice lacking LGP2 compared with controls, again indicative of earlier robust host defense responses in the $Lgp2^{-/-}$ mice (Fig. 7*F*). Thus, the loss of LGP2 augments resistance to VSV infection, plausibly by allowing RIG-I to exert an enhanced ability to stimulate the production of type I IFN and suppress infection.

Loss of LGP2 represses IFN induction in response to EMCV

To further complement these studies, we analyzed the effect of EMCV infection, a positive stranded virus, in MEFs lacking LGP2. MDA5, rather than RIG-I, has been shown to be essential for recognizing EMCV infection and triggering type I IFN production (19, 22). Our data indicated no significant differences in EMCV viral replication or in the induction of type I IFN when comparing infected WT MEFs to LGP2-lacking MEFs (Fig. 8*A*). Plausibly, this may be due to EMCV being able to avoid triggering host defense responses in these cells. However, a more dramatic effect was observed when infecting LGP2-deficient macrophages. Surprisingly, in this situation a defect in type I IFN production was observed following EMCV infection in LGP2-lacking cells compared with controls (Fig. 8*B*). A corresponding increase in viral titers was observed in LGP2-deficient macrophages, presumably due to the lack of IFN production (Fig. 8*C*). Similar observations were found following the infection of BMDCs obtained from $Lgp2^{-/-}$mice (Fig. 8*D*). To further analyze the consequences of EMCV infection in the absence of LGP2, we infected $Lgp2^{-/-}$ or control mice i.v. with 1×10^7 PFU/mouse ($n = 4$). At 4 and 24 h postinfection, serum was taken from the animals and selected cytokine levels were measured by ELISA. This analysis indicated that IFN-β, IFN-α, and IL-6 levels were dramatically reduced in animals lacking LGP2 following EMCV infection (Fig. 8, *E–G*). Furthermore, whereas VSV was able to modestly induce CD83 in $LGP2^{-/-}$ BMDCs compared with WT cells, the expression of this marker did not significantly differ following infection with EMCV (Fig. 8*H*). Animals lacking LGP2 also exhibited less resistance to lethal i.p. EMCV infection (100 PFU/animal; $n = 10$) (Fig. 8*I*) compared with WT control animals. $Lgp2^{-/-}$ mice infected i.v. with EMCV showed defective induction of IP-10 and MIG (monokine induced by IFN-γ) after 4 h in an analysis of its serum using a cytokine array (10^7 PFU/mouse; $n = 3$) (Fig. 8*J*). Collectively, these analyses indicate that a loss of LGP2 can significantly influence host innate immune responses depending on the type of virus. Plausibly, LGP2 is required for efficient antiviral responses following EMCV infection, a signaling process requiring MDA5. In contrast, the loss of LGP2 augments type I IFN production in response to transfected poly(I:C) or VSV, the latter of which activates RIG-I-mediated host defense responses.

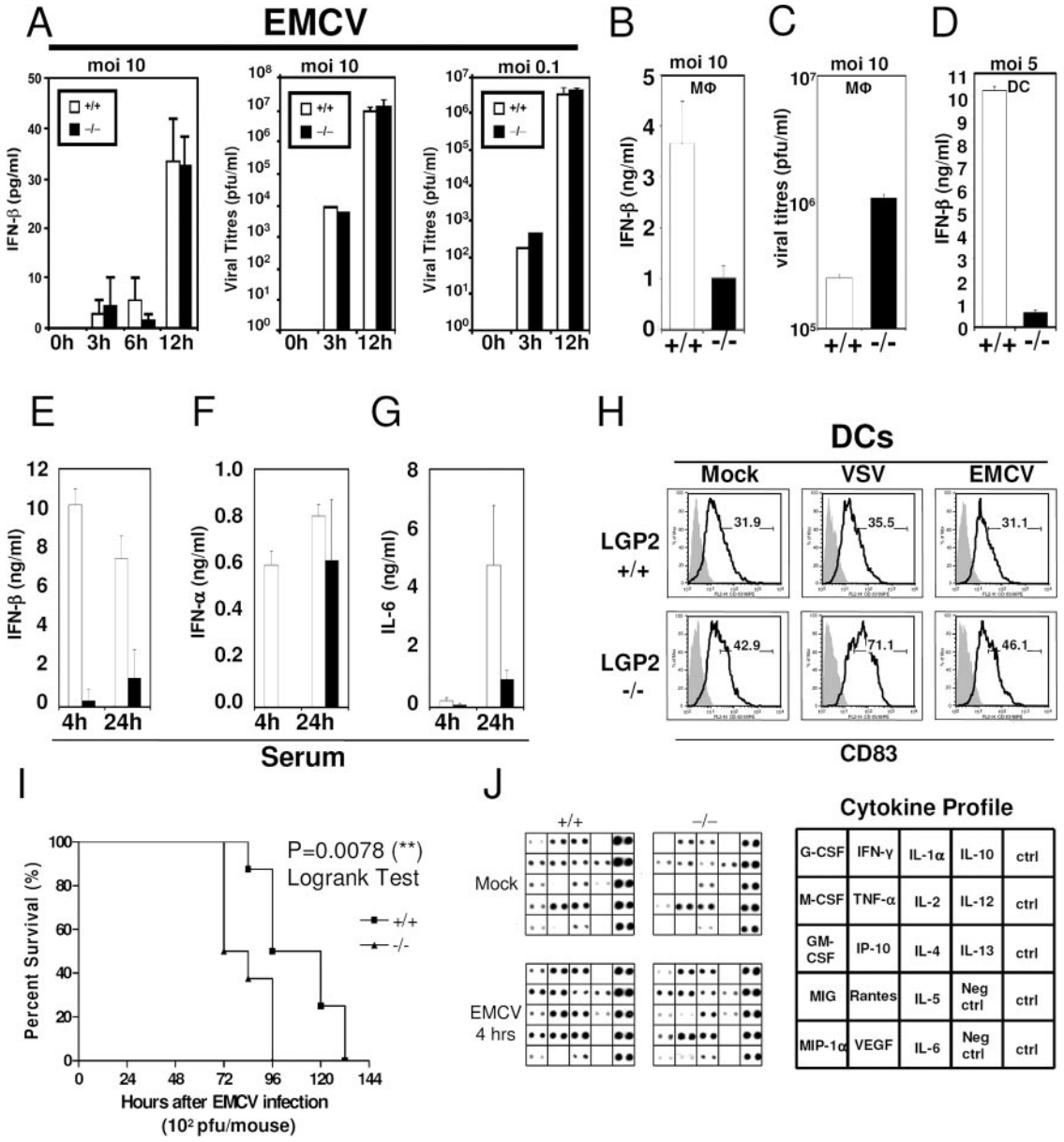

FIGURE 8. The effect of EMCV infection on cells and mice lacking LGP2. *A*, Analysis of IFN-β protein by ELISA from medium in control or *Lgp2*$^{-/-}$ cells infected with EMCV (MOI of 10) for the indicated time points. Viral titers from the same supernatant (MOI of 10) and from cells infected at MOI of 0.1 were measured by plaque assay. *B*, Macrophages (Mϕ) were infected with EMCV (MOI of 10) and IFN-β levels were measured after 24 h. *C*, Progeny EMCV yield in the supernatant of the same experiment as in *B*. *D*, BMDCs were infected with EMCV (MOI of 5) and IFN-β levels were measured after 24 h. *E–G*, Serum levels of IFN-β, IFN-α, and IL-6 in mice infected with EMCV (10^7 PFU/mouse i.v., $n = 4$). *H*, BMDCs isolated from *Lgp2*$^{+/+}$ and *Lgp2*$^{-/-}$ mice were infected with VSV and EMCV at MOI of 10 and DC maturation was observed by measuring CD83 expression levels by flow cytometry. *I*, Survival curve of mice infected with EMCV (10^2 PFU/mouse, i.p.). *J*, Cytokine profiles of *Lgp2*$^{+/+}$ and *Lgp2*$^{-/-}$ mice infected with or without EMCV (10^7 pfu/mouse i.v., $n = 3$). After 4 h, serum was collected from the mice and the cytokine profile was measured. Analysis was done in triplicate per group, and the results of one typical experiment are shown.

Discussion

The DExD/H box helicases MDA5 and RIG-I, responsible for facilitating host defense countermeasures in response to virus infection, appear to be expressed at low constitutive levels in the absence of type I IFN. Presumably, RIG-I and MDA5 serve as stress sentinels ready to recognize virus invasion (1). Following infection with positive- or negative-stranded viruses, MDA5 or RIG-I, respectively, trigger a signaling cascade culminating in the production of *IFN-*β and other genes in the so-called primary innate immune response pathway. Both RIG-I and MDA5, but not strongly LGP2, are primary innate immune response genes and thus rapidly induce themselves in response to intracellular viral RNA species before the production of type I IFN, the engagement of the JAK/STAT pathway, and the production of numerous genes that contain a cognate IFN-stimulated response element in their promoter regions (1, 39). However, RIG-I and MDA5 are also IFN inducible and thus these proteins can further stimulate their own transcription in an autologous positive feedback manner. In the presence of virus infection, this positive feedback loop would remain engaged unless virus infection was eliminated or cell death ensued. In vitro evidence has indicated that the DExD/H helicase LGP2, which lacks a CARD domain harbored by RIG-I and MDA5, may exert an inhibitory role on the ability of both RIG-I and MDA5 to induce the production of type I IFN in response to dsRNA (32). Previous evidence would

indicate that LGP2 becomes induced by type I IFN and exercises a negative regulatory effect on MDA5 and/or RIG-I function. The mechanism of this repressor action has been reported to involve the sequestration of RNA activators that would normally associate with RIG-I and MDA5 to activate CARD-mediated signaling (32, 34). A further report indicted that LGP2 may block RIG-I and MDA5 by forming a protein complex with IPS-1 (35). However, a recent study indicated that LGP2 only exhibited strong inhibitory function against RIG-I and not against MDA5. LGP2 exerted this activity by binding directly to RIG-I through a repressor domain (40). Plausibly, this event could control RIG-I association with IPS-1 via their respective CARD domains.

Collectively, our data presented here, derived by using MEFs or animals lacking LGP2, indicate that *IFN-β* mRNA production by poly(I:C) is increased in vitro compared with controls. Further, the heterologous expression of RIG-I and MDA5 can exert a more potent ability to induce type I IFN in the absence of LGP2 following the addition of transfected poly(I:C). These data would be consistent with the notion that LGP2 can negatively regulate the ability of RIG-I and MDA5 to induce type I IFN in response to poly(I:C). Recently, it has been reported that RIG-I is able to recognize ssRNA bearing 5-phosphates such as those produced from viruses like VSV (24). Cells lacking RIG-I have been demonstrated to lack the ability to stimulate the production of type I IFN following infection with VSV, a negative-stranded virus, but not EMCV, a positive-stranded virus (19). However, MDA5 has been shown to be essential for recognizing EMCV infection and in vitro transcribed RNA for reasons that remain to be fully clarified. In macrophages, MDA5 has also been shown to be essential for recognizing poly(I:C) (22). Our data demonstrate that in MEFs the heterologous expression of RIG-I or MDA5 potently stimulates type I IFN production in response to transfected poly(I:C). These observations could infer that heterogeneous RNA species within poly(I:C) preparations may activate both MDA5 and RIG-I pathways, as other have also shown (19, 22). Our observations further demonstrate that in the absence of LGP2, the ability of both RIG-I and MDA5 to stimulate the production of type I IFN is greatly increased. Thus, at least in response to poly(I:C), the loss of LGP2 can augment the production of type I IFN. This may be due to an in vitro artifact or may indicate that RIG-I and MDA5 can both respond to transfected poly(I:C), at least in MEFs. Alternatively, endogenous MDA5 may be able to form heterodimers with RIG-I to stimulate IFN production and the further synthesis of MDA5. Tissue-specific regulatory factors may additionally play a factor in regulating dsRNA-mediated signaling events. Further, LGP2 may indeed sequester RNA species and/or bind to and inhibit downstream effector molecules such as IPS-1.

A more complex picture regarding the function of LGP2 in innate signaling responses became apparent following the infection of LGP2$^{-/-}$ cells or mice with different RNA viruses. First, we observed that the induction of type I IFN was slightly augmented in LGP2$^{-/-}$ cells following infection with VSV. These data would concur with the notion that LGP2 is a negative regulator of RIG-I function and would agree with our experiments using transfected poly(I:C). Further, we demonstrate that mice lacking LGP2 are less sensitive to lethal i.n. VSV infection compared with control animals. Type I and II IFN levels were undetectable in the serum of mice inoculated i.n. by day 5, indicating that the infection is contained and likely localized to the olfactory region (38). However, we did observe significant differences in IL-12 levels in animals infected i.n. IL-12 has been proposed to promote recovery from lethal VSV infection of the CNS through a variety of mechanisms (38, 41). In addition to these data, direct i.v. inoculation with VSV also resulted in a slight increase in IFN-β levels by 24 h in *Lgp2*$^{-/-}$ animals compared with controls and a significant difference in IFN-γ levels (not observed systemically after 5 days following i.n. infection). IFN-γ has been demonstrated to inhibit VSV replication in neurons in part through the stimulation of NO production, which exerts direct antiviral effects and can modulate signal transduction pathways associated with cytokine production (42). In addition, both IL-12 and IFN-γ similarly exert direct antiviral activity and are potent regulators of the adaptive immune response (41, 43). LGP2 could further influence viral clearance by stimulating levels of type I IFN production that, aside from exerting direct antiviral activity, is critical for the generation of effector and memory T cells and can influence Ab responses to viral infection (44, 45).

In contrast with data obtained using VSV, we observed that LGP2$^{-/-}$ cells and animals actually had a defective ability to produce type I IFN following exposure to EMCV. Accordingly, animals lacking LGP2 were more sensitive to lethal EMCV infection. These data would again be in accordance with the notion that LGP2 predominantly represses the RIG-I pathway rather than the MDA5 pathway, however, indicating a potential positive regulatory role in the recognition of EMCV (40). Preliminary data indicate that the heterologous expression of LGP2 can inhibit VSV infection but not EMCV infection (data not shown). The mechanisms of RIG-I specific repression may include the direct association of LGP2 with RIG-I to prevent latent activity. Alternatively, LGP2 may associate with a downstream effector molecule such as IPS-1, although in this scenario it may be expected that LGP2 would inhibit both MDA5 and RIG-I, which we do not observe, at least under our experimental conditions. In such a situation, unrepressed RIG-I may compete with MDA5 for downstream effectors, reducing the ability of MDA5 to respond to specific virus infection. It may also be plausible that LGP2 is a cofactor for MDA5, as well as a repressor of RIG-I, because the binding of MDA5 to LGP2 in vitro has been reported (40). It is not clear why RIG-I would be preferentially regulated negatively by LGP2 rather than MDA5. Perhaps these molecules are able to coassociate in innateosome complexes that have evolved to respond to different viruses. A loss of selected molecules could effect the regulation of such responses following association with different RNA types. Clearly, further work will be required to clarify these issues.

Finally, our data indicate that the negative feedback inhibition of *IFN-β* transcription in response to poly(I:C) also occurred in the absence of LGP2, suggesting that this helicase is not significantly responsible for suppressing the poly(I:C)-triggered IFN-β pathway. In addition, *Lgp2*$^{-/-}$ animals treated with exogenous poly(I:C) (noncomplexed) did not exhibit any enhanced ability to rapidly produce type I IFN compared with controls, presumably because this pathway is governed by the TLR pathway, which is independent of RIG-I and MDA5 (17–19). The negative feedback inhibition of type I IFN production by exogenous poly(I:C) in vivo similarly occurred in *Lgp2*$^{-/-}$ animals, suggesting that LGP2 does not robustly affect the TLR 3 or TLR 7/8 pathway. Collectively, our data indicate that LGP2 restrains the activity of RIG-I early after exposure to viruses such as the VSV species, presumably because this may avoid repression of the MDA5 pathway or may avoid deleterious inflammatory responses occurring as a consequence of robust RIG-I activity (46). However, the mechanism that prevents an unconstrained poly(I:C)-activated positive feedback loop, dependent on RIG-I and MDA5, likely involves molecules other than LGP2.

Acknowledgments

We thank T. Fujita for anti-LGP2 and anti-RIG-I serum, P. B. Fisher for anti-MDA5 serum, and J. Durbin for STAT1-deficient cells. We also thank S. Balachandran for technical assistance.

Disclosures

The authors have no financial conflict of interest.

References

1. Akira, S., S. Uematsu, and O. Takeuchi. 2006. Pathogen recognition and innate immunity. *Cell* 124: 783–801.
2. Medzhitov, R., and C. A. Janeway, Jr. 1997. Innate immunity: the virtues of a nonclonal system of recognition. *Cell* 91: 295–298.
3. Ferrandon, D., J. L. Imler, and J. A. Hoffmann. 2004. Sensing infection in *Drosophila*: Toll and beyond. *Semin. Immunol.* 16: 43–53.
4. Leclerc, V., and J. M. Reichhart. 2004. The immune response of *Drosophila melanogaster*. *Immunol. Rev.* 198: 59–71.
5. Iwasaki, A., and R. Medzhitov. 2004. Toll-like receptor control of the adaptive immune responses. *Nat. Immunol.* 5: 987–995.
6. Oshiumi, H., M. Matsumoto, K. Funami, T. Akazawa, and T. Seya. 2003. TICAM-1, an adaptor molecule that participates in Toll-like receptor 3-mediated interferon-β induction. *Nat. Immunol.* 4: 161–167.
7. Beutler, B. 2004. Inferences, questions and possibilities in Toll-like receptor signalling. *Nature* 430: 257–263.
8. O'Neill, L. A., K. A. Fitzgerald, and A. G. Bowie. 2003. The Toll-IL-1 receptor adaptor family grows to five members. *Trends Immunol.* 24: 286–290.
9. Yamamoto, M., S. Sato, H. Hemmi, S. Uematsu, K. Hoshino, T. Kaisho, O. Takeuchi, K. Takeda, and S. Akira. 2003. TRAM is specifically involved in the Toll-like receptor 4-mediated MyD88-independent signaling pathway. *Nat. Immunol.* 4: 1144–1150.
10. Yamamoto, M., S. Sato, K. Mori, K. Hoshino, O. Takeuchi, K. Takeda, and S. Akira. 2002. Cutting edge: a novel Toll/IL-1 receptor domain-containing adapter that preferentially activates the IFN-β promoter in the Toll-like receptor signaling. *J. Immunol.* 169: 6668–6672.
11. Ishida, T., S. Mizushima, S. Azuma, N. Kobayashi, T. Tojo, K. Suzuki, S. Aizawa, T. Watanabe, G. Mosialos, E. Kieff, et al. 1996. Identification of TRAF6, a novel tumor necrosis factor receptor-associated factor protein that mediates signaling from an amino-terminal domain of the CD40 cytoplasmic region. *J. Biol. Chem.* 271: 28745–28748.
12. Cao, Z., W. J. Henzel, and X. Gao. 1996. IRAK: a kinase associated with the interleukin-1 receptor. *Science* 271: 1128–1131.
13. Muzio, M., J. Ni, P. Feng, and V. M. Dixit. 1997. IRAK (Pelle) family member IRAK-2 and MyD88 as proximal mediators of IL-1 signaling. *Science* 278: 1612–1615.
14. Suzuki, N., S. Suzuki, G. S. Duncan, D. G. Millar, T. Wada, C. Mirtsos, H. Takada, A. Wakeham, A. Itie, S. Li, et al. 2002. Severe impairment of interleukin-1 and Toll-like receptor signalling in mice lacking IRAK-4. *Nature* 416: 750–756.
15. Kawai, T., and S. Akira. 2006. Innate immune recognition of viral infection. *Nat. Immunol.* 7: 131–137.
16. Sato, S., M. Sugiyama, M. Yamamoto, Y. Watanabe, T. Kawai, K. Takeda, and S. Akira. 2003. Toll/IL-1 receptor domain-containing adaptor inducing IFN-β (TRIF) associates with TNF receptor-associated factor 6 and TANK-binding kinase 1, and activates two distinct transcription factors, NF-κB and IFN-regulatory factor-3, in the Toll-like receptor signaling. *J. Immunol.* 171: 4304–4310.
17. Lund, J. M., L. Alexopoulou, A. Sato, M. Karow, N. C. Adams, N. W. Gale, A. Iwasaki, and R. A. Flavell. 2004. Recognition of single-stranded RNA viruses by Toll-like receptor 7. *Proc. Natl. Acad. Sci. USA* 101: 5598–5603.
18. Diebold, S. S., T. Kaisho, H. Hemmi, S. Akira, and C. Reis e Sousa. 2004. Innate antiviral responses by means of TLR7-mediated recognition of single-stranded RNA. *Science* 303: 1529–1531.
19. Kato, H., O. Takeuchi, S. Sato, M. Yoneyama, M. Yamamoto, K. Matsui, S. Uematsu, A. Jung, T. Kawai, K. J. Ishii, et al. 2006. Differential roles of MDA5 and RIG-I helicases in the recognition of RNA viruses. *Nature* 441: 101–105.
20. Yoneyama, M., M. Kikuchi, T. Natsukawa, N. Shinobu, T. Imaizumi, M. Miyagishi, K. Taira, S. Akira, and T. Fujita. 2004. The RNA helicase RIG-I has an essential function in double-stranded RNA-induced innate antiviral responses. *Nat. Immunol.* 5: 730–737.
21. Kang, D. C., R. V. Gopalkrishnan, Q. Wu, E. Jankowsky, A. M. Pyle, and P. B. Fisher. 2002. *mda*-5: An interferon-inducible putative RNA helicase with double-stranded RNA-dependent ATPase activity and melanoma growth-suppressive properties. *Proc. Natl. Acad. Sci. USA* 99: 637–642.
22. Gitlin, L., W. Barchet, S. Gilfillan, M. Cella, B. Beutler, R. A. Flavell, M. S. Diamond, and M. Colonna. 2006. Essential role of *mda-5* in type I IFN responses to polyriboinosinic:polyribocytidylic acid and encephalomyocarditis picornavirus. *Proc. Natl. Acad. Sci. USA* 103: 8459–8464.
23. Kato, H., S. Sato, M. Yoneyama, M. Yamamoto, S. Uematsu, K. Matsui, T. Tsujimura, K. Takeda, T. Fujita, O. Takeuchi, and S. Akira. 2005. Cell type-specific involvement of RIG-I in antiviral response. *Immunity* 23: 19–28.
24. Hornung, V., J. Ellegast, S. Kim, K. Brzozka, A. Jung, H. Kato, H. Poeck, S. Akira, K. K. Conzelmann, M. Schlee, et al. 2006. 5′-Triphosphate RNA is the ligand for RIG-I. *Science* 314: 994–997.
25. Pichlmair, A., O. Schulz, C. P. Tan, T. I. Naslund, P. Liljestrom, F. Weber, and C. Reis e Sousa. 2006. RIG-I-mediated antiviral responses to single-stranded RNA bearing 5′-phosphates. *Science* 314: 997–1001.
26. Kawai, T., K. Takahashi, S. Sato, C. Coban, H. Kumar, H. Kato, K. J. Ishii, O. Takeuchi, and S. Akira. 2005. IPS-1, an adaptor triggering RIG-I- and Mda5-mediated type I interferon induction. *Nat. Immunol.* 6: 981–988.
27. Meylan, E., J. Curran, K. Hofmann, D. Moradpour, M. Binder, R. Bartenschlager, and J. Tschopp. 2005. Cardif is an adaptor protein in the RIG-I antiviral pathway and is targeted by hepatitis C virus. *Nature* 437: 1167–1172.
28. Seth, R. B., L. Sun, C. K. Ea, and Z. J. Chen. 2005. Identification and characterization of MAVS, a mitochondrial antiviral signaling protein that activates NF-κB and IRF 3. *Cell* 122: 669–682.
29. Xu, L. G., Y. Y. Wang, K. J. Han, L. Y. Li, Z. Zhai, and H. B. Shu. 2005. VISA is an adapter protein required for virus-triggered IFN-β signaling. *Mol. Cell* 19: 727–740.
30. Balachandran, S., E. Thomas, and G. N. Barber. 2004. A FADD-dependent innate immune mechanism in mammalian cells. *Nature* 432: 401–405.
31. Takahashi, K., T. Kawai, H. Kumar, S. Sato, S. Yonehara, and S. Akira. 2006. Roles of caspase-8 and caspase-10 in innate immune responses to double-stranded RNA. *J. Immunol.* 176: 4520–4524.
32. Yoneyama, M., M. Kikuchi, K. Matsumoto, T. Imaizumi, M. Miyagishi, K. Taira, E. Foy, Y. M. Loo, M. Gale, Jr., S. Akira, et al. 2005. Shared and unique functions of the DExD/H-box helicases RIG-I, MDA5, and LGP2 in antiviral innate immunity. *J. Immunol.* 175: 2851–2858.
33. Cui, Y., M. Li, K. D. Walton, K. Sun, J. A. Hanover, P. A. Furth, and L. Hennighausen. 2001. The Stat3/5 locus encodes novel endoplasmic reticulum and helicase-like proteins that are preferentially expressed in normal and neoplastic mammary tissue. *Genomics* 78: 129–134.
34. Rothenfusser, S., N. Goutagny, G. DiPerna, M. Gong, B. G. Monks, A. Schoenemeyer, M. Yamamoto, S. Akira, and K. A. Fitzgerald. 2005. The RNA helicase Lgp2 inhibits TLR-independent sensing of viral replication by retinoic acid-inducible gene-I. *J. Immunol.* 175: 5260–5268.
35. Komuro, A., and C. M. Horvath. 2006. RNA and virus-independent inhibition of antiviral signaling by RNA helicase LGP2. *J. Virol.* 80: 12332–12342.
36. Komiyama, Y., S. Nakae, T. Matsuki, A. Nambu, H. Ishigame, S. Kakuta, K. Sudo, and Y. Iwakura. 2006. IL-17 plays an important role in the development of experimental autoimmune encephalomyelitis. *J. Immunol.* 177: 566–573.
37. Faria, P. A., P. Chakraborty, A. Levay, G. N. Barber, H. J. Ezelle, J. Enninga, C. Arana, J. van Deursen, and B. M. Fontoura. 2005. VSV disrupts the Rae1/mrnp41 mRNA nuclear export pathway. *Mol. Cell* 17: 93–102.
38. Komatsu, T., M. Barna, and C. S. Reiss. 1997. Interleukin-12 promotes recovery from viral encephalitis. *Viral Immunol.* 10: 35–47.
39. Stetson, D. B., and R. Medzhitov. 2006. Type I interferons in host defense. *Immunity* 25: 373–381.
40. Saito, T., R. Hirai, Y. M. Loo, D. Owen, C. L. Johnson, S. C. Sinha, S. Akira, T. Fujita, and M. Gale, Jr. 2007. Regulation of innate antiviral defenses through a shared repressor domain in RIG-I and LGP2. *Proc. Natl. Acad. Sci. USA* 104: 582–587.
41. Trinchieri, G. 2003. Interleukin-12 and the regulation of innate resistance and adaptive immunity. *Nat. Rev. Immunol.* 3: 133–146.
42. Chesler, D. A., C. Dodard, G. Y. Lee, D. E. Levy, and C. S. Reiss. 2004. Interferon-γ-induced inhibition of neuronal vesicular stomatitis virus infection is STAT1 dependent. *J. Neurovirol.* 10: 57–63.
43. Shtrichman, R., and C. E. Samuel. 2001. The role of γ interferon in antimicrobial immunity. *Curr. Opin. Microbiol.* 4: 251–259.
44. Le Bon, A., C. Thompson, E. Kamphuis, V. Durand, C. Rossmann, U. Kalinke, and D. F. Tough. 2006. Cutting edge: enhancement of antibody responses through direct stimulation of B and T cells by type I IFN. *J. Immunol.* 176: 2074–2078.
45. Thompson, L. J., G. A. Kolumam, S. Thomas, and K. Murali-Krishna. 2006. Innate inflammatory signals induced by various pathogens differentially dictate the IFN-I dependence of CD8 T cells for clonal expansion and memory formation. *J. Immunol.* 177: 1746–1754.
46. De Clercq, E., and P. De Somer. 1975. Are cytotoxicity and interferon inducing activity of poly(I).poly(C) invariably linked in interferon-treated L cells? *J. Gen. Virol.* 27: 35–44.